

# Trade-off analysis for structural design of high-precision space reflector using multiobjective optimization method

著者	Kodama Ryo, Kogiso Nozomu, Toyoda Masahiro, Tanaka Hiroaki
journal or publication title	Mechanical Engineering Journal
volume	2
number	4
page range	15-00058
year	2015-08-15
権利	(c) 2015 The Japan Society of Mechanical Engineers
URL	<a href="http://hdl.handle.net/10466/15697">http://hdl.handle.net/10466/15697</a>

doi: 10.1299/mej.15-00058

# Trade-off analysis for structural design of high-precision space reflector using multiobjective optimization method

Ryo KODAMA\*, Nozomu KOGISO\*, Masahiro TOYODA\* and Hiroaki TANAKA\*\*

\* Department of Aerospace Engineering, Osaka Prefecture University

1-1 Gakuen-Cho, Naka-Ku, Sakai, Osaka 599-8531, Japan

E-mail: kogiso@aero.osakafu-u.ac.jp

\*\* Department of Aerospace Engineering, National Defence Academy of Japan

1-10-20 Hashirimizu, Yokosuka, Kanagawa 239-8686, Japan

Received XX January 2015

## Abstract

This study investigates the robustness of a space reflector structure consisting of radial ribs and hoop cables by using the multiobjective optimization method. The radial ribs are deformed into a parabola shape by cable tensions applied to the hoop cables that are arranged concentrically around the central hub and to the tie cables that are connected to the deployable structure. The design problem is to achieve the ideal deformation shape for the radial rib under the prescribed cable tensions through the determination of the rib height distribution. In addition, the ability to adjust the shape by changing the cable tension is required for handling uncertainty under actual environment condition. A simplified structural model with only one radial rib is used for structural design, where the cables are replaced by equivalent tensions. This study adopts the multiobjective optimization method to verify the structural design by investigating the trade-off between the deformation error and its sensitivity with respect to the cable tensions. Robustness corresponds to lower value of sensitivity, that the RMS error is difficult to deteriorate by changing the cable tension. On the other hand, design with higher value of sensitivity is called adjustability, because such a design is easy to adjust the deformation shape by the cable tension. The primary objective of the design problem is to minimize the RMS error between the ideal and the deformation shape of the rib under the prescribed cable tension in terms of the rib dimensions. The other two objectives are to accomplish the robustness and the adjustability of the rib deformation shape by adjusting the cable tension using the tie cable and the outermost hoop cable. This multiobjective optimization problem is evaluated by the satisficing trade-off method (STOM). Through investigating Pareto solutions obtained from the two-objective and then the three-objective function problems, the effects of cable tension variations on the surface shape error and the robustness are discussed.

**Key words** : High-precision space structure, Uncertainty, Multiobjective optimization, Satisficing trade-off method, Structural design verification, Trade-off analysis, Nonlinear finite element method.

## 1. Introduction

Space antenna for space exploration missions require large aperture area and high surface shape accuracy, as well as lightweightness. The radial rib and hoop cable structure for the space reflector as illustrated in Fig. 1 [Higuchi et al., 2009, Tanaka et al., 2011, Miyazaki and Tanaka, 2011] was proposed to satisfy these difficult requirements. The ribs are arranged in the radial direction from a central hub, hoop cables are connected to the radial ribs and arranged concentrically, and tie cables are connected between the rib and the backup deployable truss. The ribs are deformed to the ideal parabola shape by cable tension upon deployment, where they are originally straight upon folding.

The structural design is verified through the one-dimensional rib model shown in Fig. 2 [Tanaka et al., 2011]. The one-dimensional model consists of a single rib taken from the whole reflector and a cable element that represents the tie cable. The root of the rib is simply supported, and the lower end of the tie cable is fixed in the vertical direction and free

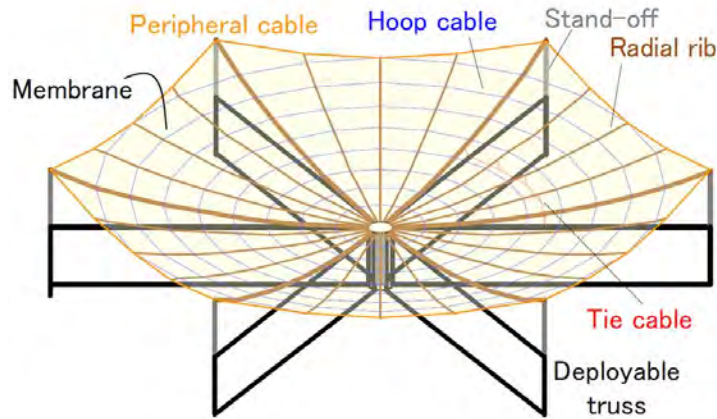


Fig. 1 Radial-rib/hoop cable reflector structure [Miyazaki and Tanaka, 2011]. The radial ribs are connected to the backup deployable structure at a central hub and circumference stand-off struts. The hoop cables are arranged concentrically around the central hub and the tie cables are connected to the deployable structure. The radial ribs are deformed into an ideal parabola shape by the cable tension upon deployment.

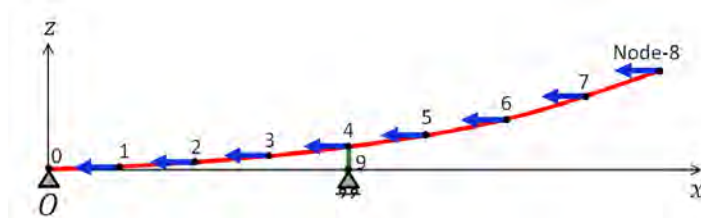


Fig. 2 Simplified one-dimensional structural model of the rib/cable reflector consisting of the single rib that is taken from the whole reflector. The root of the rib is simply supported and the hoop cable tension is modeled as a nodal load while the tie cable is modeled by a cable element and the tension is applied as the reaction force on the rib deformation. The rib dimension and the unstressed length of the tie cable are treated as design variables.

to move in the longitudinal direction. The hoop cable tension is modeled as a concentrated nodal load that deforms the rib into the ideal parabola shape from the original straight form. The deformation transmits the tension force to the tie cable as a reaction force.

In the conventional model described in reference [Tanaka et al., 2011], the tie cable is modeled as an equivalent nodal force instead of a cable element, whereas the longitudinal direction is fixed at the rib tip. Then, the structural shape is designed to remove the reaction force at the tip end. It is difficult to use this method for investigating the effect of tip hoop cable variations by changing the hoop cable load because the conventional model should make the reaction force at the rib tip vanish by the finite element method. Therefore, the one-dimensional model is modified to remove the tip constraint and introduce the tie cable element as shown in Fig. 2. The other constraint imposed is that the cable element should not be slackened in the design verification.

The structural design problem is to determine the rib height distribution in order to minimize the RMS error between the ideal parabola shape and the rib deformation shape by the given applied loads, which is evaluated by the nonlinear finite element method. The design problem can be formulated as an optimization problem, where the rib dimensions and the unstressed length of the tie cable are treated as design variables. In addition, this study investigates the effect of the cable tension on the rib deformation and the RMS error minimization design. Under actual situations, material properties or the applied load have uncertainties that will cause variation in rib deformation from the ideal shape. In that case, the deformation will be corrected by changing the cable tension. The adjustability is accomplished by increasing the RMS error sensitivity with respect to the cable tension. On the other hand, a smaller sensitivity increases the rib structure robustness upon variations of the cable tension. The design with lower RMS error sensitivity value with respect to the cable tension and lower RMS error is called the robust design in this study. The robust design is generally defined as the design with the smallest deterioration in performance under a variety of uncertain design parameters, as well as a reasonable higher performance [Park et al., 2006, Beyer and Sendhoff, 2007].

The objective of this study is to investigate the design problem, especially the trade-off between the RMS error and the RMS sensitivity with respect to the cable tension. For this purpose, the design problem is formulated as a multiob-

jective optimization problem [Mittinen, 2004]. Then, the trade-off analysis is performed by investigating the Pareto set distributions. This study adopts the satisficing trade-off method (STOM) [Nakayama and Sawaragi, 1984] as the multi-objective optimization method. STOM can obtain a single, highly accurate Pareto solution, regardless of the shape of the Pareto set. Therefore, the method is widely applied to engineering design problems [Nakayama et al., 1995, Okamoto et al., 2014]. Some of the authors developed robust and reliability-based multiobjective optimization methods considering uncertainty using STOM [Toyoda and Kogiso, 2015, Kogiso et al., 2014]. By introducing an aspiration level that corresponds to the user's preference for each objective function, STOM transforms the multiobjective optimization problem into an equivalent single-objective problem. Mathematical programming techniques can be applied to the transformed problem, meaning that STOM obtains a Pareto solution efficiently. In addition, a highly diverse and uniformly distributed Pareto set can be obtained by parametrically changing the aspiration level. STOM is an interactive approach because the search process is repeated by changing the aspiration level until the user is satisfied with the solution. The automatic trade-off analysis method [Nakayama, 1992] is one way of updating the aspiration level using sensitivity information.

Regarding the multiobjective optimization, it is also important to select a suitable design candidate among the Pareto solutions. A data-mining method using a self-organizing map [Obayashi and Sasaki, 2003] is one of the resolving methods that figure out some useful relationship among Pareto solutions. This method is widely used in engineering design problems to extract design information from the Pareto set [Okamoto et al., 2014, Oyama et al., 2010]. A method using clustering analysis is another visualizing method that makes clear the trade-off among Pareto solutions. This method has been applied to engineering design problems such as turbine blade [Jeong et al., 2005] and automobile body structure design [Kohira and Amano, 2014].

These visualization methods are used to evaluate the trade-off after obtaining all possible Pareto solutions. In this study, the range of design candidates is narrowed interactively along with increasing the number of objective functions. The primary objective of the design is to satisfy the RMS error limit of the rib deformation. First, the RMS error minimized design is obtained as a reference design by applying a single-objective optimization. Then, multiobjective optimization is applied to investigate the trade-off between the RMS error and its sensitivities with respect to the cable tensions, where the RMS error and its sensitivity with respect to the tie cable tension or the outermost hoop cable tension are used as the two competitive objective functions. Uniformly distributed Pareto sets in both objective optimization problems are obtained by parametrically changing the aspiration level. Through the trade-off analysis, the design range is narrowed to the range of interest. Then, three objective optimization problems, including RMS error and both sensitivities, are performed to restrict the aspiration level to the design range of interest. Finally, the trade-off analysis is performed through the obtained few Pareto solutions. This approach is applied to the three types of rib design studies. The first is a robust design that minimizes the three objective functions, i.e., the RMS error and the two sensitivities. Then, the adjustability of the rib structure is investigated using two design strategies; either the tie cable or the outermost hoop cable is used as the adjuster. The design problems are formulated as maximizing the RMS error sensitivity with respect to the adjuster cable tension and minimizing the RMS error itself and the other RMS error sensitivity. The validity of the design studies through the trade-off analysis is discussed.

## 2. Multiobjective Optimal Design

A multiobjective optimization problem is an optimization problem with multiple objective functions.

$$\mathbf{f}(\mathbf{x}) = [f_1(\mathbf{x}), f_2(\mathbf{x}), \dots, f_k(\mathbf{x})]^T \quad (1)$$

where  $k$  is the number of objective functions,  $\mathbf{x} = (x_1, x_2, \dots, x_{n_x})^T$  are the design variables, and  $n_x$  is the number of design variables.

The multiobjective optimization problem is generally formulated as follows:

$$\begin{aligned} \text{Minimize: } & \mathbf{f}(\mathbf{x}) = [f_1(\mathbf{x}), f_2(\mathbf{x}), \dots, f_k(\mathbf{x})]^T \\ \text{subject to: } & g_j(\mathbf{x}) \leq 0 \quad (j = 1, \dots, m) \\ & x_i^L \leq x_i \leq x_i^U \quad (i = 1, \dots, n_x) \end{aligned} \quad (2)$$

where  $g_j(\mathbf{x})$  ( $j = 1, \dots, m$ ) are constraint conditions, and  $x_i^U$  and  $x_i^L$  are the upper and lower limits of the design variables, respectively.

In this study, the three objective functions are defined as the RMS error and the RMS error sensitivities with respect to the tie cable tension and the hoop cable tension in terms of the rib height and the unstressed length of the tie cable.

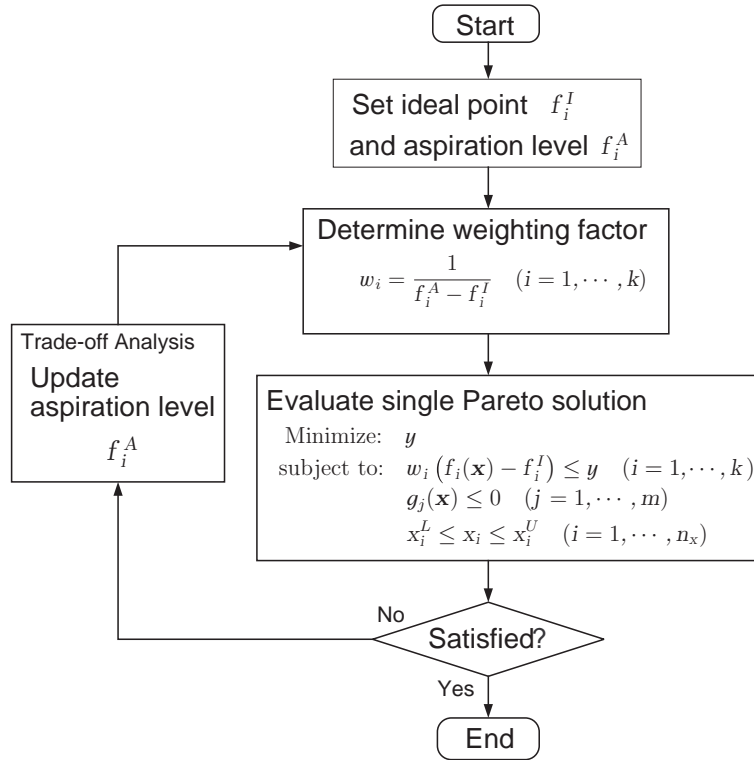


Fig. 3 Flowchart of STOM. First, set the ideal point  $f_i^I$  and the aspiration level  $f_i^A$ . Then, evaluate the weighting factor  $w_i$ . The multiobjective optimization problem is formulated as a single-objective optimization based on STOM. The Pareto solution is obtained using a nonlinear mathematical programming method. If the obtained Pareto solution does not satisfy the user, the optimization is repeated after the aspiration level  $f_i^A$  has been updated. The automatic trade-off analysis is one method of determining the aspiration level.

Then, the three design studies are formulated to investigate the trade-off between the RMS error and the sensitivities. One is the robust design that minimizes all objective functions. The others are the adjustability designs that maximizes one sensitivity and minimizes the RMS error and the other sensitivity. This problem does not have constraints except for the side constraints. The detail formulation is described in section 3.2.

### 2.1. Satisficing Trade-off Method (STOM)

STOM is known to be an interactive optimization method that converts a multiobjective optimization problem into the equivalent single-objective optimization problem by introducing an aspiration level that corresponds to the user's preference for each objective function value. The flow of STOM is summarized in Fig. 3 and briefly described as follows.

**Step 1** Set the ideal point  $f_i^I$  ( $i = 1, \dots, k$ ) of each objective function. The ideal point is usually determined by solving a single-objective optimization problem considering only the corresponding objective function  $f_i(\mathbf{x})$ . The ideal point for the mean performance is obtained by solving the deterministic design problem. As an alternative, the ideal solution without solving the optimization problem can be used such as zero to the ideal point. In this study, the ideal point of the RMS error is set as the single objective optimization. On the other hand, the ideal points are set to zero for the RMS error sensitivities.

**Step 2** Set the aspiration level  $f_i^A$  ( $i = 1, \dots, k$ ) of each objective function and evaluate the weight coefficient,  $w_i$ , as follows:

$$w_i = \frac{1}{f_i^A - f_i^I} \quad (i = 1, \dots, k) \tag{3}$$

**Step 3** Formulate the multiobjective optimization problem in Eq. (2) into the weighted Tchebyshev norm problem as follows:

$$\text{Minimize: } \max_{i=1, \dots, k} w_i (f_i(\mathbf{x}) - f_i^I) \tag{4}$$

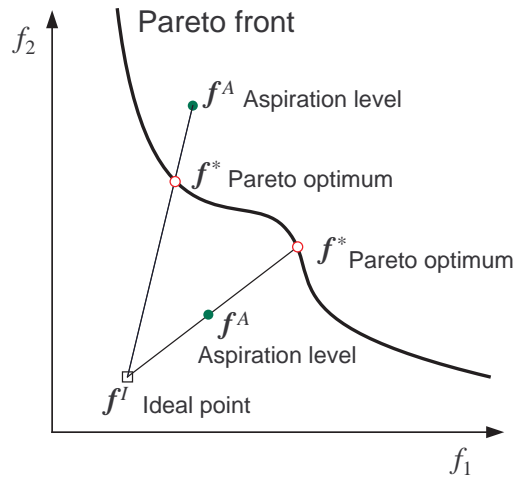


Fig. 4 Pareto solution search process of STOM described in the objective function space. The Pareto solution  $f^*$  is obtained as the intersection between the Pareto surface and the line connecting the ideal point  $f^I$  and the aspiration level  $f^A$ .

$$\begin{aligned} \text{subject to: } & g_j(\mathbf{x}) \leq 0 \quad (j = 1, \dots, m) \\ & x_i^L \leq x_i \leq x_i^U \quad (i = 1, \dots, n_x) \end{aligned}$$

**Step 4** The min-max problem in Eq. (4) is transformed into the equivalent single-objective problem by introducing a slack design variable  $y$  as follows:

$$\begin{aligned} \text{Minimize: } & y \tag{5} \\ \text{subject to: } & w_i (f_i(\mathbf{x}) - f_i^I) \leq y \quad (i = 1, 2, \dots, k) \\ & g_j(\mathbf{x}) \leq 0 \quad (j = 1, \dots, m) \\ & x_i^L \leq x_i \leq x_i^U \quad (i = 1, \dots, n_x) \end{aligned}$$

When Eq. (5) is solved using a nonlinear programming method such as a sequential programming method, an accurate Pareto optimal solution is obtained in comparison with an evolutionary method.

**Step 5** If the objective function values are satisfactory, the search is completed. Otherwise, update the aspiration level  $f_i^A$  and return to Step 2. The automatic trade-off analysis method [Nakayama, 1992] is one of the methods used to reasonably update the aspiration level.

The weight coefficient,  $w_i$ , plays an important role in obtaining the Pareto solution in the direction of the aspiration level, which is directly related to the designer's preference. As shown in Fig. 4, the Pareto optimal solution is usually located on the line connecting the ideal point and the aspiration level in the objective function space, regardless of whether or not the aspiration level lies in the feasible region. On the other hand, the optimal solution is often not located on the line when some constraints are active. In that case, designers can investigate the effect of the active constraints on the Pareto optimal solution.

An accurate Pareto set is obtained by parametrically changing the aspiration level. Designers can investigate the desired region in detail only by arranging the aspiration level properly without obtaining the full Pareto set.

### 3. Design Problem

#### 3.1. Structural model validation through ideal deformation shape design

The original design problem [Tanaka et al., 2011] was formulated as a deterministic optimization problem in order to determine the rib height distribution under the prescribed tension. In this study, the two-dimensional simple model shown in Fig. 2 is used to evaluate the deformation shape by a nonlinear finite element method. The objective function is the RMS error between the deformation shape and an ideal deformation shape, which is defined as follows:

$$v = u^2/16 \tag{6}$$

Table 1 Rib unstressed length and cable tension for the simplified structural model shown in Fig. 2. Details are given in reference [Tanaka et al., 2011].

(a) Rib properties								
Section	0-1	1-2	2-3	3-4	4-5	5-6	6-7	7-8
Unstressed length (m)	0.25254	0.25279	0.25327	0.25400	0.25500	0.25620	0.25760	0.25930

(b) Hoop cable tension applied at nodal force to the left direction								
Node	1	2	3	4	5	6	7	8
Load (N)	0.4187	1.0467	1.0467	1.0467	1.0467	1.0467	2.0934	2.0934

Table 2 Deterministic optimal solution and side constraints for RMS error minimization design. The design is used as the reference design in the multiobjective optimization problems described in section 3.2.

(a) Rib thickness										
Position	0-0.5	0.5-1	1-2	2-3	3-4	4-5	5-6	6-7	7-7.5	7.5-8
Lower limit (mm)	2.5	3.0	4.0	4.0	4.0	4.0	4.0	4.0	2.5	2.0
Optimum height (mm)	2.96	3.87	4.84	5.50	5.96	5.85	5.12	4.13	2.89	2.37

(b) Tie cable unstressed length	
	Tie cable length
Upper limit (mm)	70.0
Optimum length (mm)	63.67

where  $u$  is the longitudinal coordinate and  $v$  is the bending deformation.

The rib is modeled by using 80 beam elements, such that the rib between each node in Fig. 2 is equally divided into 10 beam elements. The tie cable is modeled as a single cable element. The root of the rib is simply supported and the bottom end of the tie cable is fixed in the height direction but is free to move in the lateral direction. The hoop cable tension values are given as the equivalent nodal force, as listed in Table 1. The tie cable tension is given as a reaction force resulting from the rib deformation, where the Young’s modulus of the rib and the cable stiffness are set to constants as 70 GPa and 2000 N, respectively.

In the optimization problem, the beam height is treated as a design variable, where the beam cross section is assumed to be a rectangular shape and the beam width is set to be constant at 5 mm. The design variables are allocated such that the beam elements between each node have the same beam height except for the two ends. Both ends allocate two variables such that the elements between the nodes are divided into two equal parts, and then each variable allocates each of the five elements on the left- and right-hand sides. Hence, the number of the beam height variables is 10. In addition, the unstressed length of the cable element is treated as a design variable. The length indirectly affects the rib deformation shape to change the cable tension that is represented as the reaction force. As a result, the total number of design variables is 11.

For numerical stability, the lower limits of the rib heights are imposed as listed in Table 2(a). In addition, the upper limit of the tie cable unstressed length is given as listed in Table 2(b) to avoid slackening of the tie cable. It is confirmed that no limits are active for this optimization or the following multiobjective optimization problems.

Using the simple model, the RMS error minimization design is obtained as shown in Table 2. The obtained RMS error is 0.0288mmRMS, which satisfies the design requirement of 0.05mmRMS [Tanaka et al., 2011]. The deformation error from the ideal deformation shape in Eq. (6) is illustrated in Fig. 5. The error is zigzagged between the nodes because the rib height is constant between the nodes. It is found that the error range is set within  $\pm 0.07$  mm by separating the design variables at the root and tip ends of the rib.

The structural model described herein is different from that in the original study [Tanaka et al., 2011]. In the original study, the tie cable was not modeled as the tie cable element. The cable tension was given as the nodal force at rib node 4 in the vertical direction and the lateral direction was fixed at the rib tip. The optimization was performed to minimize RMS error, as well as to reduce the reaction force at the tip. It is difficult to use this model for evaluating the effect of variations of the cable tension on the rib deformation, which is why the current study updates the structural model to that shown in Fig. 2. The difference between the obtained results and the previous results [Tanaka et al., 2011] is very small. The RMS error is 0.037mmRMS and the difference of the rib height distribution is small. For the above reasons, this structural model is considered adequate for the current purpose.

### 3.2. Formulation of multiobjective optimization problem

The deformation RMS error minimization is not the only design requirement; the RMS error sensitivity is also

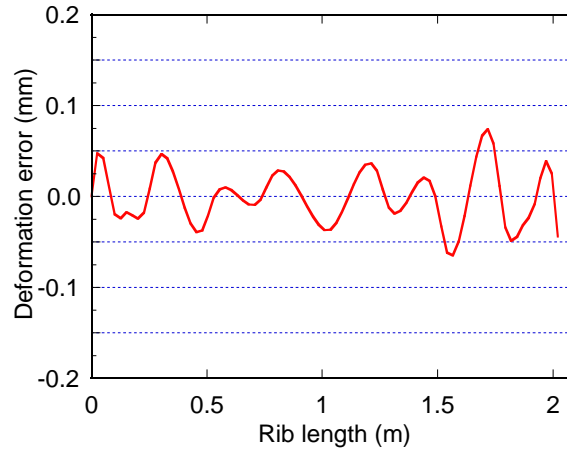


Fig. 5 Deformation error from the ideal deformation shape of the deterministic optimized rib shown in Table 2.

required in order to solve the design problem. This study focuses on the RMS error sensitivity with respect to the cable tension force as the performance measure of the shape adjustability or the robustness. The sensitivity with respect to the random variable is widely used to evaluate the performance deterioration under variation of a random variable through the first-order approximation [Ang and Tang, 1975]. The rib shape is changed by the cable tension. Therefore, the cable tension is used as the rib shape adjuster when the sensitivity with respect to the tension is large. On the other hand, the design is called robust when the sensitivity is small. The robustness or adjustability are investigated by formulating the design problem as a multiobjective optimization problem. The objective functions are described as follows:

$$f_1 = \text{Deformation RMS error from the ideal deformation shape (mm)} \tag{7}$$

$$f_2 = \text{RMS error sensitivity with respect to tension of the tie cable at node 4 (mm/N)} \tag{8}$$

$$f_3 = \text{RMS error sensitivity with respect to tension of the outermost hoop cable at node 8 (mm/N)} \tag{9}$$

where sensitivity with respect to the cable tension is evaluated by the following forward difference:

$$\frac{\partial \text{RMS}(x, z)}{\partial z_i} \approx \frac{\text{RMS}(x, z + \Delta z_i) - \text{RMS}(x, z)}{\Delta z_i} \tag{10}$$

where  $z$  denotes the design parameters as the cable tension. The perturbed value  $\Delta z_i$  is set as 0.1% of the nominal cable tension, that is determined to confirm the numerical stability referred from our previous research [Kogiso et al., 2011]. Maximization of  $f_2$  or  $f_3$  corresponds to the achievement of adjustability of the rib deformation by changing the corresponding cable tension. On the other hand, minimization of  $f_2$  or  $f_3$  corresponds to the robust design.

This study considers the following three design strategies formulated as a multiobjective optimization problem, where the RMS error  $f_1$  is minimized for all three cases to accomplish the ideal deformation shape:

**Design study 1 (Minimize  $f_1$ ,  $f_2$  and  $f_3$ )** The objective is to achieve robustness upon variations of the tie cable and the outermost hoop cable tensions.

**Design study 2 (Minimize  $f_1$  and  $f_2$  and maximize  $f_3$ )**  $f_3$  is maximized to use the outermost hoop cable connected to node 8 as an adjuster. At the same time,  $f_2$  is minimized to achieve robustness upon variation of the tie cable tension.

**Design study 3 (Minimize  $f_1$ , maximize  $f_2$  and minimize  $f_3$ )**  $f_2$  is maximized to use the tie cable connected to node 4 as the adjuster. At the same time,  $f_3$  is minimized to achieve robustness upon variation of the outermost hoop cable tension.

### 3.3. Verification sequence

As described above, the design requirement for the RMS error corresponding to  $f_1$  is set as less than 0.05mmRMS [Tanaka et al., 2011]. However, the reference values of the RMS error sensitivity have not been referred. Therefore, the design verification is performed in the following sequence to clarify the effect of variation of cable tension on the rib deformation.

Table 3 Reference design as RMS error minimization design. This design is obtained from the RMS error  $f_1$  minimization.  $f_2$  and  $f_3$  are RMS error sensitivity with respect to the outermost cable tension and the tie cable tension, respectively.

Objective	$f_1$ (mmRMS)	$f_2$ (mm/N)	$f_3$ (mm/N)
Reference value	0.0288	66.0	27.8

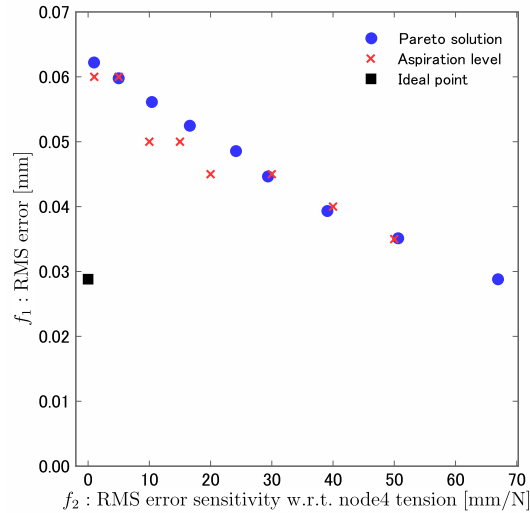


Fig. 6 Pareto set distribution in  $f_2$ - $f_1$  space for the two-objective function problem in design study 1: Minimize deformation error as RMS error ( $f_1$ ) and RMS error sensitivity with respect to the tie cable tension ( $f_2$ ). Note that this Pareto set is also a part of the Pareto set in design study 2.

**Step 1** A single-objective optimization problem to minimize the deformation RMS error  $f_1$  is obtained first. The optimum design listed in Table 3 is used as the reference design. Values of the objective functions on the reference design are listed in Table 2.

**Step 2** Two-objective optimization problems consisting of  $f_1$  and  $f_2$  or  $f_1$  and  $f_3$  are performed. The aspiration levels are parametrically changed to obtain a highly diverse and uniformly distributed Pareto set. Then, it is evaluated in terms of how much the sensitivity is improved by sacrificing the RMS error within the allowable range.

**Step 3** Finally, three-objective optimization problem considering all objective functions  $f_1$ ,  $f_2$  and  $f_3$  is evaluated, where the aspiration levels are limited to only the range of interest from the previous step. Then, the effect of variations of cable tension on the rib deformation is discussed.

Investigating only a limited number of three-objective optimum designs using properly determined aspiration levels is the major advantages of STOM for design verification. It is also effective to save the computational cost.

## 4. Design Verifications

### 4.1. Design study 1

The respective initial Pareto solutions obtained from the two objective function problems of this example are shown in Figs. 6 and 7, where the two objectives are to minimize  $f_1$  and  $f_2$ , and  $f_1$  and  $f_3$ , respectively. The lower rightmost Pareto solution in both Figs. 6 and 7 corresponds to the reference point as listed in Table 3. Both Pareto curves show the trade-off relationship between  $f_1$  and  $f_2$ , and  $f_1$  and  $f_3$ . That is, the RMS error increases as the RMS error sensitivity decreases. Within the allowable range of an RMS error lower than 0.05mmRMS,  $f_2$  and  $f_3$  decrease by as much as approximately 20 mm/N and 3 mm/N, respectively.

These Pareto points are obtained by parametrically changing the aspiration levels, where the  $f_1$ - $f_2$  and the  $f_1$ - $f_3$  problems use eight and six aspiration levels as shown in Figs. 6 and 7, respectively. These points are initially selected from the reference points; later, the aspiration level can set as close to the Pareto point as desired. The dotted line in Fig. 7 indicates the connecting line from the ideal point to the aspiration level, showing that the found Pareto solution lies on the line. This corresponds to the characteristics of STOM shown in Fig. 4.

Then, the three-objective design problem to minimize  $f_1$ ,  $f_2$  and  $f_3$  is solved by setting the aspiration levels, referring to the results of the two-objective problems above. The Pareto solutions plot in  $f_2$ - $f_3$  space is shown in Fig. 8. The values

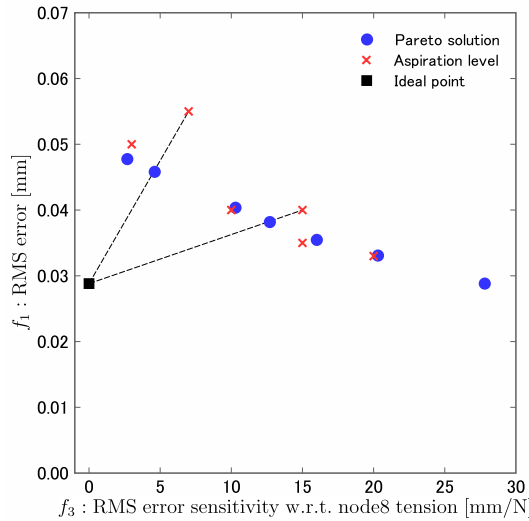


Fig. 7 Pareto set distribution in  $f_3$ - $f_1$  space for the two objective function problem in design study 1: Minimize deformation error as RMS error ( $f_1$ ) and RMS error sensitivity with respect to the outermost hoop cable tension ( $f_3$ ). The dotted lines connect the ideal point and the aspiration level. It is found that the Pareto solution lies on the line. Note that this Pareto set is also a part of the Pareto set in design study 3.

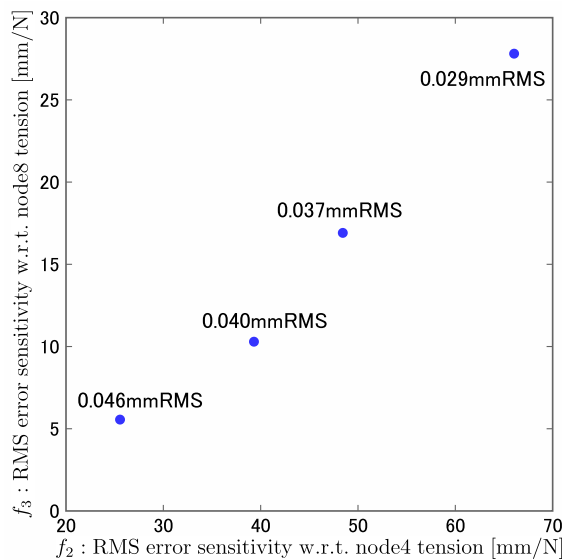


Fig. 8 Pareto solution for the three-objective optimization problem in design study 1: Minimize  $f_1$ ,  $f_2$  and  $f_3$ . The Pareto solutions described in  $f_2$ - $f_3$  space and the values of  $f_1$  are given in the figure. Meaningful designs are those in the lower left from the reference design indicated as 0.029mmRMS.

correspond to the RMS error  $f_1$ . The upper rightmost point of 0.029mmRMS corresponds to the reference design listed in Table 2. The Pareto solution distribution in Fig. 8 shows that  $f_2$  and  $f_3$  have a strong correlation and the possibility of improvement of  $f_2$  and  $f_3$  by sacrificing the RMS error  $f_1$  within the allowable range.

#### 4.2. Design study 2

This design study corresponds to the outermost hoop cable tension made adjustable to the rib shape by maximizing the RMS error sensitivity with respect to the cable tension  $f_3$ , in addition to minimizing the RMS error  $f_1$  and the RMS error sensitivity with respect to the tie cable tension  $f_2$ . The Pareto set of the two-objective problem that combines minimization of  $f_1$  and maximization of  $f_3$  is shown in Fig. 9. The two objectives also have a trade-off relationship, as seen with objectives  $f_1$  and  $f_2$  in the Pareto set shown in Fig. 6. The RMS error rapidly deteriorates as the sensitivity  $f_3$  increases beyond 35 mm/N. That is, the upper limit of  $f_3$  should be 35 mm/N.

The Pareto set for the three-objective problem is shown in Fig. 10, where the aspiration levels are determined from the Pareto set for the two-objective problems. As in the last section, the Pareto set is plotted in  $f_2$ - $f_3$  space and the values

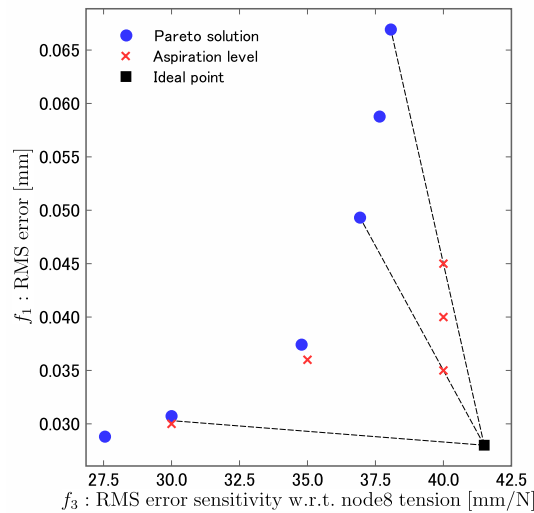


Fig. 9 Pareto set distribution in  $f_3$ - $f_1$  space for the two-objective function problem in design study 2: Minimize deformation error as RMS error ( $f_1$ ) and maximize RMS error sensitivity with respect to the outermost hoop cable tension ( $f_3$ ). The dotted lines connect the ideal point and the aspiration level. It is found that the Pareto solution lies on the line.

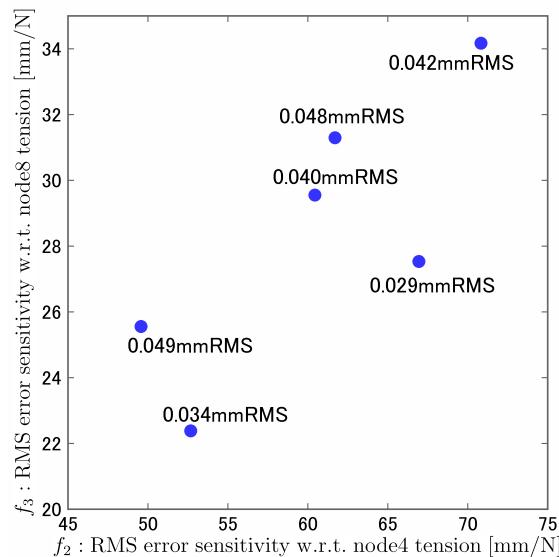


Fig. 10 Pareto solution for  $f_1$ ,  $f_2$  and  $f_3$  in design study 2: Minimize  $f_1$  and  $f_2$  and maximize  $f_3$ . The Pareto solutions described in  $f_2$ - $f_3$  space and the value of  $f_1$  are given in the figure.

of the RMS error  $f_1$  are shown in the figure. The right middle point 0.029mmRMS indicates the reference design. From the plotted Pareto designs, only the two designs plotted in the upper left from the reference design 0.048mmRMS and 0.040mmRMS, improve both sensitivity function values  $f_2$  and  $f_3$  by sacrificing the RMS error  $f_1$ . It is found that the improvement is very small. From the obtained Pareto set, the achievement of this design strategy is very difficult and inefficient.

### 4.3. Design study 3

In contrast to the above example, this design study corresponds to the tie hoop cable tension made adjustable to the rib shape by maximizing the RMS error sensitivity with respect to the cable tension  $f_2$  in addition to minimizing the RMS error  $f_1$  and the RMS error sensitivity with respect to the outermost hoop cable tension  $f_3$ . The Pareto set of the two-objective problems combining the minimization of  $f_1$  and maximization of  $f_2$  is shown in Fig. 9. It is found that the RMS error rapidly deteriorates as the sensitivity value  $f_2$  increases beyond 80 N/mm. The Pareto set for the two-objective functions to minimize  $f_1$  and  $f_3$  is shown in Fig. 7.

Then, the three-objective functions problem is evaluated by considering the results of the two-objective optimization

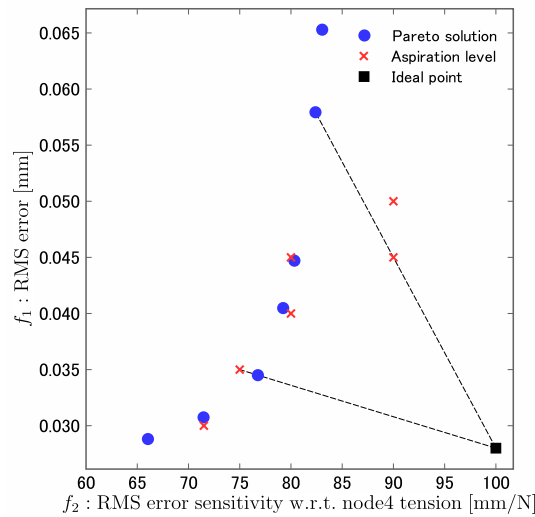


Fig. 11 Pareto solutions described in  $f_2$ - $f_1$  space for the two-objective function problem in design study 3: Minimize deformation error as RMS error ( $f_1$ ) and maximize RMS error sensitivity with respect to the tie cable tension ( $f_2$ ). The dotted lines connect the ideal point and the aspiration level. It is found that the Pareto solution lies on the line.

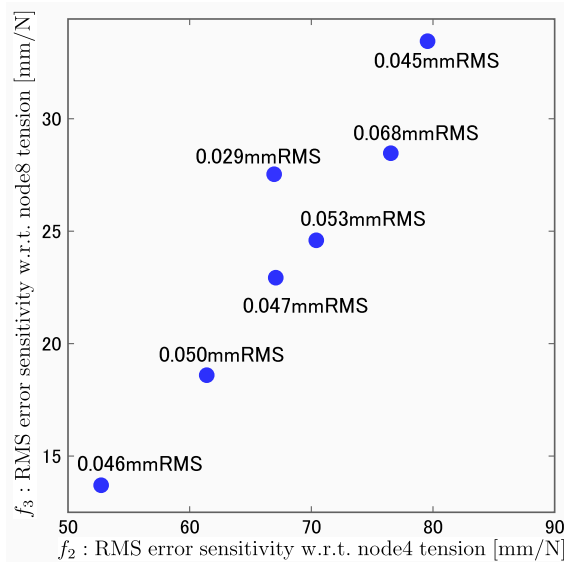


Fig. 12 Pareto solution for  $f_1, f_2$  and  $f_3$  in design study 3: Minimize  $f_1$  and  $f_3$  and maximize  $f_2$ . The Pareto solutions described in  $f_2$ - $f_3$  space and the value of  $f_1$  are given in the figure

problems. The obtained Pareto set in  $f_2$ - $f_3$  space is illustrated in Fig. 12. As in the examples above, the design with 0.029mmRMS corresponds to the reference design. The only efficient designs are the two in the lower right from the reference point, i.e., 0.047mmRMS and 0.053mmRMS; however, the improvement is very small. Further improvement should sacrifice the RMS error  $f_1$ . As in design strategy 2, this strategy is not efficient.

**4.4. Summary of design studies**

From these studies, we are able to obtain robust designs that minimized both RMS error sensitivity with respect to the tie cable and the outermost hoop cables, as shown in design study 1. However, as shown in design studies 2 and 3, it is difficult to obtain designs satisfying both robustness for cable tension and shape adjustability.

To investigate the difference between the obtained Pareto solutions, differences of the deformation error are shown in Fig. 13. Here, the deformation RMS error is minimized in all design cases. In total, four two-objective design problems are evaluated: (i) minimize  $f_1$  and  $f_2$  in design studies 1 and 2, (ii) minimize  $f_1$  and  $f_3$  in design studies 1 and 3, (iii) minimize  $f_1$  and maximize  $f_3$  in design study 2, and (iv) minimize  $f_1$  and maximize  $f_2$  in design study 3. There are four Pareto designs at opposite sides of the minimization of  $f_1$ , the reference design. Figure 13 shows the difference of the

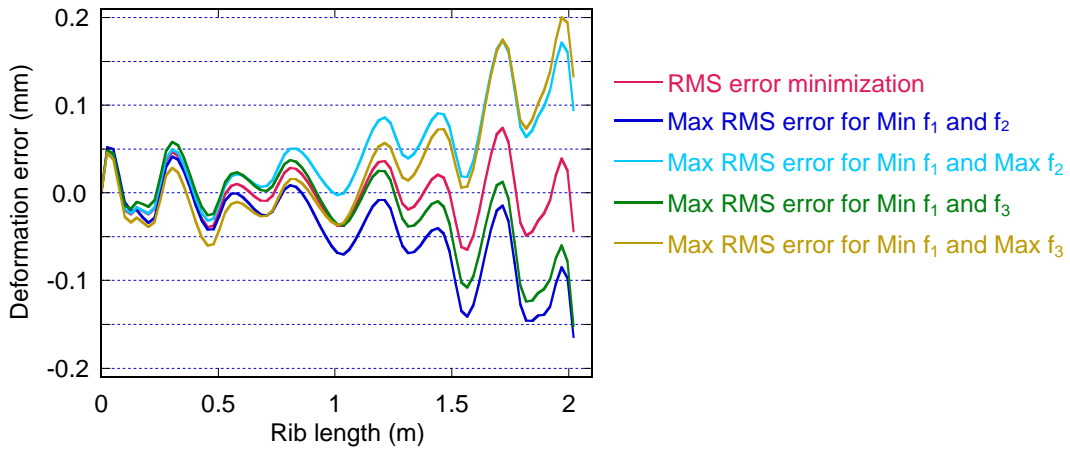


Fig. 13 Deformation error distribution for each design problem. “RMS error minimization” corresponds to the reference design obtained as the single-optimization design problem. The other four designs are the RMS error maximum designs obtained for the four two-objective optimizations, where  $f_1$  is the RMS error and  $f_2$  and  $f_3$  are the error sensitivity. For example, the second plot is the RMS error distribution for the minimization of  $f_2$  obtained from the minimization of  $f_1$  and  $f_2$ .

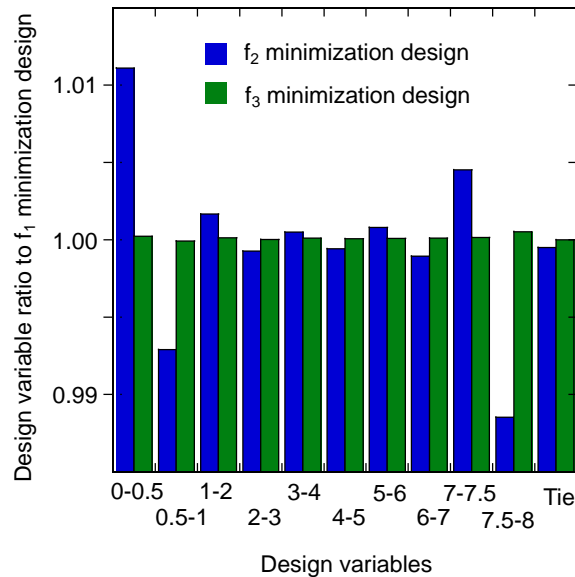


Fig. 14 Design variable ratios between  $f_2$  or  $f_3$ -minimized Pareto solutions and  $f_1$  minimization design in design study 1. The numbered horizontal values correspond to the rib height and “Tie” in the rightmost term refers to the unstressed length of the tie cable.

deformation error distributions between the reference design and the four designs. Comparing the reference design, the two designs that minimize  $f_2$  or  $f_3$  are shifted in the negative direction. On the other hand, the other two designs that maximize  $f_2$  or  $f_3$  are shifted in the positive direction.

In addition to variation of cable tensions, it is important to investigate the effect of variations in the dimensions. Figure 14 shows the design variable ratios on the basis of the  $f_1$ -minimized single-objective design shown in Table 2 and for the  $f_2$  and  $f_3$  minimization designs for the two-objective problems in design study 1. Note that the difference is very small for both the rib heights and the tie cable tension.

Finally, the RMS error sensitivity with respect to the rib height for the reference design is investigated. The results obtained by forward difference is shown in Fig. 15, where the horizontal axis indicates the node number. The sensitivity is small at both the root and the tip but extremely high elsewhere. This high sensitivity is in agreement with the results shown in Fig. 14. The maximum value is 13.9mmRMS/mm between nodes 3 and 4. These results mean that every 0.01 mm change in rib height deteriorates the deformation RMS error by as much as 0.139mmRMS, which is much higher than the upper limit, 0.05mmRMS. Therefore, the rib requires extremely high manufacturing accuracy.

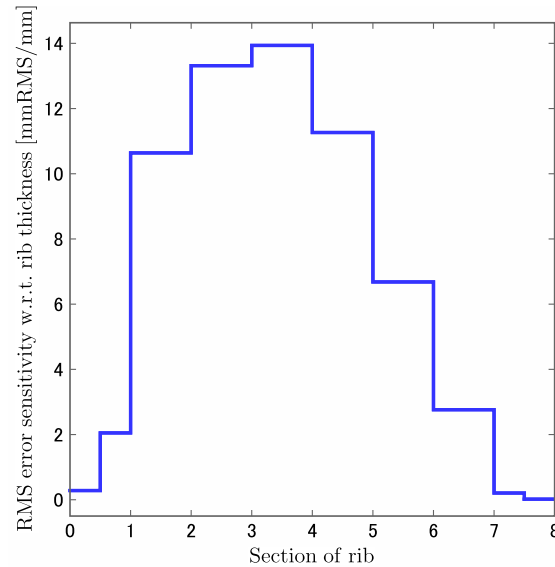


Fig. 15 RMS error sensitivity with respect to rib height distribution for the reference design. Horizontal axis corresponds to the node numbers given in Fig. 2.

## 5. Conclusions

This study verifies the structural design considering uncertainties of a space reflector structure consisting of radial ribs and hoop cables by using the multiobjective optimization method. Deformation RMS error with respect to the accuracy of rib deformation and RMS sensitivities with respect to cable tension, i.e., the outermost hoop cable and the tie cable, are selected as objective functions to investigate the trade-off between the deformation accuracy and variations of the cable tension. STOM is adopted as numerically efficient multiobjective optimization method.

Although the upper limit of the RMS error has been determined from previous studies [Higuchi et al., 2009, Tanaka et al., 2011], the target values of the sensitivity terms have not been described clearly. Therefore, a three-step approach is adopted. First, single-objective optimization is performed to minimize the RMS error; the obtained optimum design is regarded as the reference value. Then, two sets of two-objective optimization, one including the RMS error and the other including the sensitivity, are performed to investigate the Pareto set distributions. Finally, the Pareto solutions of a three-objective optimization problem are obtained to investigate the trade-off relationship, where the aspiration levels are determined from results of the two-objective problems.

Three design studies are investigated. One is a robust design that minimizes the RMS error and the two sensitivity terms. In the other two designs, the sensitivity term is maximized in order to use the outermost hoop cable (Strategy 2) or the tie cable (Strategy 3) as the deformation control adjuster while the RMS error and the other sensitivity term are minimized. Through the design studies, the following conclusions are remarked:

- As shown in design study 1, it is useful to obtain robust designs that minimize both RMS error sensitivity terms with respect to the tie cable and the outermost hoop cables.
- As shown in design studies 2 and 3, however, it is difficult to obtain designs satisfying both the robustness for cable tension and the shape adjustability.
- The obtained Pareto designs are very sensitive to the rib dimensions. Therefore, such ribs require extremely high manufacturing accuracy.

The obtained results are much more difficult than we expected for design of high-precision space structure. However, the quantitative trade-off results themselves are useful on the design process. This is a significant advantage of our proposed trade-off analysis method based on STOM.

## Acknowledgment

This study is partially supported by JSPS KAKENHI 26249131.

## References

- Ang, A. H.-S. and Tang, W. H., Probabilistic concepts in engineering design, basic principles, (1975), Wiley.
- Beyer, H. and Sendhoff, B., Robust optimization – a comprehensive survey, *Computer Methods in Applied Mechanics and Engineering*, Vol. 196, No. 33-34 (2007), pp. 3190-3218, doi:10.1016/j.cma.2007.03.003
- Higuchi, K., Kishimoto, N., Meguro, A., Tanaka, H., Yoshihara, M. and Iikura, S., Structure of high precision large deployable reflector for space VLBI (very long baseline interferometry), *Proceedings of 50th AIAA/ASME/ASCE/AHS/ASC Structures, Structural Dynamics, and Materials Conference*, AIAA-2009-2609 (2009), pp. 1-9.
- Jeong, M. J., Dennis, B. H. and Yoshimura, S., Multidimensional clustering interpretation and its application to optimization of coolant passages of a turbine blade, *Journal of Mechanical Design*, Vol. 127, No. 2, (2005), pp. 215-221, doi:10.1115/1.1830047
- Kogiso, N., Tanaka, H., Akita, T., Ishimura, K., Sakamoto, H., Ogi, Y., Miyazaki, Y. and Iwasa, T., Comparison of computation accuracy in FEM analysis for a space antenna structural design, *Proceedings of 24th JSME Computational Mechanics Conference CMD2011*, No. 2328 (2011), pp. 691-693. (in Japanese)
- Kogiso, N., Kodama, R. and Toyoda, M., Reliability-based multiobjective optimization using the satisficing trade-off method, *Journals of the Japan Society of Mechanical Engineers*, Vol. 1, No. 6 (2014), p. DSM0063, doi:10.1299/mej.2014dsm0063
- Kohira, T. and Amano, K., Knowledge discovery for car-body weight reduction with multidisciplinary design optimization and trade off analysis, *IEEJ transactions on Electronics, Information and Systems*, Vol. 134, No. 9 (2014), pp. 1348-1354, (in Japanese) doi:10.1541/ieej.iss.134.1348
- Mittinen, K. M., *Nonlinear multiobjective optimization*, (2004), Kluwer Academic Publishers.
- Miyazaki, Y. and Tanaka, H., Elastica solution for simplified model for a space antenna structure consisting of radial ribs and hoop cables, *Proceedings of 24th JSME Computational Mechanics Conference CMD2011*, No. 2327 (2011), pp. 689-690. (in Japanese)
- Nakayama, H., Trade-off analysis using parametric optimization techniques, *European Journal of Operational Research*, Vol. 60, No. 1 (1992), pp. 87-98, doi:10.1016/0377-2217(92)90336-8
- Nakayama, H., Kaneshige, K., Takemoto, S. and Watada, Y., An application of a multi-objective programming technique to construction accuracy control of cable-stayed bridges, *European Journal of Operational Research*, Vol. 87, No. 3 (1995), pp. 731-738, doi:10.1016/0377-2217(95)00241-3
- Nakayama, H. and Sawaragi, Y., Satisficing trade-off method for multiobjective programming, *Lecture Notes in Economics and Mathematical Systems*, Vol. 229 (1984), pp. 113-122, doi:10.1007/978-3-662-00184-4\_13
- Obayashi, S. and Sasaki, D., Visualization and data mining of Pareto solutions using self-organizing map, *Lecture Notes in Computer Science*, Vol. 2632 (2003), pp. 796-809, doi:10.1007/3-540-36970-8\_56
- Okamoto, T., Hanaoka, Y., Aiyoshi, E. and Kobayashi, Y., A buffer material optimal design in the radioactive wastes geological disposal using the satisficing trade-off method and the self-organizing map, *Electrical Engineering in Japan*, Vol. 187, No. 2 (2014), pp. 17-32, doi: 10.1002/eej.22634
- Oyama, A., Nonomura, T. and Fujii, K., Data mining of Pareto-optimal transonic airfoil shapes using proper orthogonal decomposition, *Journal of Aircraft*, Vol. 47, No. 5 (2010), pp. 1756-1762, doi:10.2514/1.C000264
- Park, G., Lee, T., Lee, K. and Hwang, K., Robust design: an overview, *AIAA Journal*, Vol. 44, No. 1 (2006), pp. 181-191, doi:10.2514/1.13639
- Tanaka, H., Akita, T., Kogiso, N., Ishimura, K., Sakamoto, H., Ogi, Y. and Miyazaki, Y., A design method for a space antenna structure consisting of radial ribs and hoop cables, *Proceedings of 24th JSME Computational Mechanics Conference CMD2011*, No. 2326 (2011), pp. 687-688. (in Japanese)
- Toyoda, M. and Kogiso, N., Robust multiobjective optimization method using satisficing trade-off method, *Journal of Mechanical Science and Technology*, Vol. 29, No. 4 (2015), pp. 1361-1367, doi: 10.1007/s12206-015-0305-9